THE JOURNAL OF PHYSICAL CHEMISTRY B

ARTICLE

pubs.acs.org/JPCB

Probing End-to-End Cyclization beyond Willemski and Fixman

Shaohua Chen and Jean Duhamel*

Institute of Polymer Research, Department of Chemistry, University of Waterloo, 200 University Avenue West, Waterloo, ON N2L 3G1, Canada

Mitchell A. Winnik

Department of Chemistry, University of Toronto, 80 St. George Street, Toronto, Ontario M5S 3H6, Canada

Supporting Information

ABSTRACT: A series of poly(ethylene oxide)s labeled at both ends with pyrene, (PEO(X)−Py_2, where X represents the number average molecular weight (M_n) of the PEO chains and equals 2, 5, 10, and 16.5 K) was prepared together with one-pyrene-monolabeled PEO (PEO(2K)−Py). The process of end-to-end cyclization (EEC) was investigated by monitoring intramolecular excimer formation in seven organic solvents with viscosities (η) ranging from 0.32 to 1.92 mPa·s. The steady-state fluorescence spectra showed that excimer formation of PEO(X)−Py_2 decreased strongly with increasing η and M_n. The monomer and excimer time-resolved fluorescence decays were analyzed according to the traditional Birks' scheme. Birks' scheme analysis indicated that the decrease in excimer formation with increasing M_n and η was due partly to a decrease in the rate constant of EEC, but most importantly, to a large increase in the fraction of pyrenes that did not form excimer (f_{Mfree}). This result is in itself incompatible with Birks' scheme analysis which requires that f_{Mfree} be the molar fraction of chains bearing a single pyrene at one chain end; in short, f_{Mfree} does not depend on M_n and η within the framework of Birks' scheme analysis. In turn, this unexpected result agrees with the framework of the fluorescence blob model (FBM) which predicts that quenching takes place inside a *blob*, which is the finite volume probed by an excited chromophore during its lifetime. Increasing M_n and η results in a larger fraction of chains having a conformation where the quencher is located outside the blob resulting in an increase in f_{Mfree}. Equations were derived to apply the FBM analysis, originally designed to study randomly labeled polymers, to the end-labeled PEO(X)−Py_2 series. FBM analysis was found to describe satisfyingly the data obtained with the longer PEO(X)−Py_2 samples.

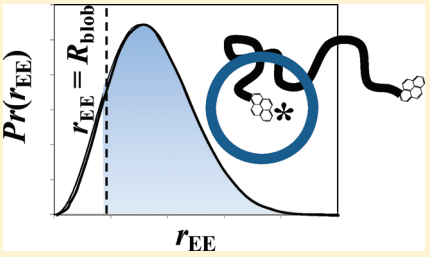

INTRODUCTION

End-to-end cyclization (EEC) experiments of polymers have been of interest since the classic theoretical description of the end-to-end cyclization probability of polymer chains by Jacobson and Stockmayer in 1950.[1] Many EEC experiments are conducted by attaching a fluorophore F and a quencher Q at the opposite ends of a polymer chain (Scheme 1). In the Willemski−Fixman formulation,[2,3] the excited fluorophore F* is quenched by Q with a single rate constant k_{cy} when internal chain dynamics bring both into proximity, within a capture volume whose radius is characteristic of the reaction distance of the two groups, typically 1 nm or less.

Many examples of this type of EEC experiment have been reported.[4−37] When EEC experiments are carried out with short peptides, they are expected to reflect the dynamics of the most basic step encountered in protein folding, namely, loop formation.[4−16] In these fluorescence experiments, quenching of F* by Q (see Scheme 1) shortens its fluorescence decay time but maintains the exponential decay profile, and this decay time τ is related to k_{cy} by the expression $\tau = (\tau_o^{-1} + k_{cy})^{-1}$, where τ_o is the natural (unquenched) lifetime of F*. Analysis of the fluorescence decays is thus straightforward and yields k_{cy}, a measure of polymer flexibility. This theoretical insight brought to the fore by Willemski and Fixman[2,3] has been confirmed by numerous experimental studies carried out on a variety of polymer backbones[4−37], which found that k_{cy} decreases with increasing number-average degree of polymerization (N_n) as $N_n^{-\alpha}$, where reported values of α range between 0.9 and 1.9.[13−20,35]

In these EEC experiments, τ_o serves as a clock that determines the time for a measurable F*−Q encounter. For long chains or slow relaxation rates, due to chain stiffness or elevated solvent viscosity, only a tiny fraction of the polymer chains in a sample will have their chain ends close enough to interact on the time scale of τ_o. Most of the excited fluorophores will not react within this time window, and the measured value of τ will be indistinguishable from τ_o. These ideas are summarized in Scheme 2, where we now focus on the radius R that describes the excursion volume sampled by the excited dye F* during its excited state. The volume sampled will be much larger for aromatic ketone[34] or anthracene[35] phosphorescence ($\tau_o \approx 100\ \mu s$) than for the fluorescence of dyes like naphthalene[36,37] or pyrene[17−32]

Received: October 4, 2010
Revised: January 14, 2011
Published: March 15, 2011

Scheme 1. EEC with the Capture Radius of the Excited Fluorophore

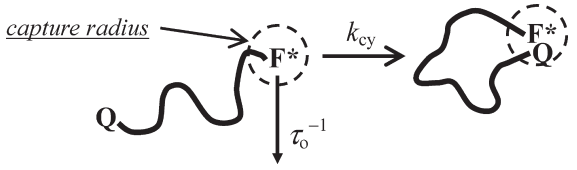

Scheme 2. EEC with the Excursion Volume of the Excited Fluorophore

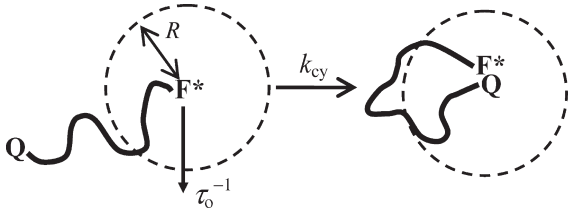

($\tau_o \approx 50-300$ ns). For fluorescent dyes and very long polymer chains, the vast majority of chain ends lie outside the excursion volume. Cyclization kinetics becomes difficult to study. Thus most experiments of this sort are carried out on polymers of short and intermediate lengths.

This observation leads to the question how the measured EEC kinetics might change under borderline conditions, where cyclization is being hindered by a long chain or a viscous solvent. If the chain is too long or the solvent too viscous, a large fraction f_{free} of the excited chromophores will decay to the ground state with a lifetime τ_o before having undergone an EEC event. EEC will occur only between those chain ends that are located sufficiently close to each other at the time of sample excitation and whose molar fraction equals $(1 - f_{free})$. As suggested in Scheme 2, the magnitude of f_{free} is expected to reflect the chain end distribution of the polymer in solution. It will also be important to distinguish this concept of f_{free} from another source of unquenchable chromophores that arise from imperfect synthesis of the labeled polymers, that small fraction of polymer chains in the sample that bear no Q.

The present study represents an attempt to investigate how f_{free} varies for a series of poly(ethylene oxide) (PEO) samples labeled at both ends with pyrene (Py) under conditions where EEC is hindered by either elevated solvent viscosity and/or sufficiently long polymer chains. Pyrene provides a particular sensitivity for the study of EEC reactions where an excited pyrene (Py*) interacts with another Py in the ground state to form an excimer (PyPy)* that has its own distinct emission.[17−32] Four monodisperse PEO samples with a number average molecular weight (M_n) value of 2000 (2K), 5000 (5K), 10 000 (10K), and 16 500 (16.5K) were labeled at both ends with Py groups. The four PEO constructs referred to as PEO(X)−Py_2 where X equals M_n were studied in seven organic solvents with viscosities ranging from 0.32 mPa·s for acetonitrile to 1.92 mPa·s for *N*, *N*-dimethylacetamide. The process of excimer formation with monodisperse end-labeled polymers is normally well-described by Birks' two-state mechanism,[38] where an extra term is added (with fraction f_{free} and pyrene monomer lifetime τ_M) to account for the small fraction of monolabeled polymers that cannot form excimer. However, our experiments lead to the surprising result that the magnitude of f_{free} increases for samples of longer chain length and for individual samples at high solvent viscosity. This strange result indicates that the magnitude of f_{free} is not linked to a fraction of chains missing a Py, but to a more fundamental feature of EEC kinetics when the fraction of cyclizing chains detected in the experiment is small. We were able to understand the nature of the phenomena by analyzing the fluorescence decay data in terms of a fluorescence blob model.

THEORY

The process of excimer formation between two pyrenes covalently attached to both ends of a monodisperse polymer has been found to be well described by Birks' scheme (Scheme 3).[17,38] Excimer formation between an excited monomer and a ground-state monomer is described by the first-order rate constant k_{cy} which depends among other factors on polymer chain length, solvent viscosity, and solvent quality toward the polymer.[17,38] Dissociation of the excimer occurs with the rate constant k_{-cy}. Excimer dissociation is usually found to be rather slow compared to the emission rate constant of the excimer τ_E^{-1} taken as the inverse of the excimer lifetime.[38] The lifetime of the pyrene monomer τ_M can be obtained with a model compound which can be the pyrene derivative used to label the polymer or, even more accurately, by using a polymer bearing a single pyrene unit.

Integration of the differential equations describing the kinetics depicted in Scheme 3 yields eqs 1 and 2 for the time-dependent concentrations of the pyrene monomer and excimer, respectively.[17,38]

$$[\mathrm{Py}^*] = \frac{[\mathrm{Py}^*_{diff}]_o}{\sqrt{(X-Y)^2 + 4k_{cy}k_{-cy}}}\left((X-\tau_2^{-1})\right.$$
$$\times \exp(-t/\tau_1) - (X-\tau_1^{-1})$$
$$\left.\times \exp(-t/\tau_2)\right) + [\mathrm{Py}^*_{free}]_o \exp(-t/\tau_M)$$
$$+ [\mathrm{Py}^*_S]_o \exp(-t/\tau_S) \quad (1)$$

$$[\mathrm{E}^*] = \frac{k_{cy}[\mathrm{Py}^*_{diff}]_o}{\sqrt{(X-Y)^2 + 4k_{cy}k_{-cy}}}\left(-\exp(-t/\tau_1)\right.$$
$$\left.+ \exp(-t/\tau_2)\right) + [\mathrm{Py}^*_S]_o \exp(-t/\tau_S) \quad (2)$$

In eqs 1 and 2, X equals $k_{cy} + \tau_M^{-1}$, Y equals $k_{-cy} + \tau_E^{-1}$, the expressions of the decay times τ_1 and τ_2 are given in eqs SI.3 and SI.4 in the Supporting Information, and $[\mathrm{Py}^*_{diff}]_o$ and $[\mathrm{Py}^*_{free}]_o$ represent the initial concentrations of pyrenes that form excimer by diffusion or do not form excimer because they are attached onto monolabeled chains, respectively.

These equations also have a term for a component of very short decay time (2−4 ns), denoted Py^*_S, not explicitly incorporated into Birks' mechanism. The species Py^*_S is encountered occasionally at wavelengths where the excimer is measured when excimer formation occurs in restricted geometries such as when the pyrene pendants are confined onto a polymer[29,30] or in a lipid bilayer.[39] In the present study, Py^*_S was observed for solutions of PEO(X)−Py_2 constructs prepared with longer chains and for samples in more viscous solvents.

Interestingly, our analysis of the monomer and excimer fluorescence decays with the above set of equations never yielded a complete set of satisfactory parameters despite the numerous

theoretical adjustments made to Birks' scheme (see the Supporting Information). In particular, the fraction of unquenched pyrenes ($f_{Mfree} = [Py^*_{free}]_o/([Py^*_{free}]_o + [Py^*_{diff}]_o)$) was found to increase with increasing polymer chain length and solvent viscosity, regardless of the model used. To account for this observation which is not predicted by Birks' scheme, the fluorescence blob model (FBM) was introduced (Scheme 4).[40,41]

The FBM assumes that, while excited, a chromophore probes a finite volume referred to as a *blob*. Excimer will form with a rate constant k_{blob} only if a ground-state pyrene manages to be in a blob together with an excited pyrene. Ground-state pyrenes can move in and out of the blob with a rate constant $k_e[M1]$ and $k_e[M0]$, respectively, where [M0] and [M1] are the concentrations of blobs that contain zero or one ground-state pyrene, respectively, and k_e is the rate constant representing the exchange of ground-state pyrenes between blobs. Assuming that $k_{-1} \ll 1/\tau_E$ (i.e., no excimer dissociation),[38] eqs 3 and 4 were derived in the Supporting Information that describe the time-dependent concentration of the pyrene monomer and excimer, respectively.

$$[Py^*] = \frac{[Py^*_{diff}]_o}{4\sqrt{\Delta}k_e([M0]+[M1])}([((k_e([M0]+[M1]) + \sqrt{\Delta})^2 - k_{blob}^2]f_M(t) \times \exp(-t/\tau_A) + [k_{blob}^2 - ((k_e([M0]+[M1]) - \sqrt{\Delta})^2]f_M(t) \times \exp(-t/\tau_B)) + [Py^*_{free}]_o f_M(t) + [Py^*_S]_o \exp(-t/\tau_S) \quad (3)$$

$$[E^*] = \frac{k_{blob}[Py^*_{diff}]_o}{4\sqrt{\Delta}k_e([M0]+[M1])} \left(-\frac{(k_{blob}+k_e[M0])^2 - (k_e[M1]+\sqrt{\Delta})^2}{\frac{1}{\tau_E} - \frac{1}{\tau_M} - \frac{1}{\tau_A}}(f_M(t) \times \exp(-t/\tau_A) - f_E(t)) + \frac{(k_{blob}+k_e[M0])^2 - (k_e[M1]-\sqrt{\Delta})^2}{\frac{1}{\tau_E} - \frac{1}{\tau_M} - \frac{1}{\tau_B}}(f_M(t) \times \exp(-t/\tau_B) - f_E(t)) \right) + [E^*]_o \times f_E(t) + [Py^*_S]_o \exp(-t/\tau_S) \quad (4)$$

The expressions of the parameters Δ, τ_A, and τ_B are given hereafter. The expressions of $f_M(t)$ and $f_E(t)$ are given in eqs 8 and 9.

$$\Delta = [k_{blob} + k_e([M0]-[M1])]^2 + 4k_e^2[M0][M1] \quad (5)$$

$$\tau_A^{-1} = \frac{1}{2}(k_{blob} + k_e([M0]+[M1]) + \sqrt{\Delta}) \quad (6)$$

$$\tau_B^{-1} = \frac{1}{2}(k_{blob} + k_e([M0]+[M1]) - \sqrt{\Delta}) \quad (7)$$

Scheme 3. Birks' Two-State Model for Py Excimer Formation

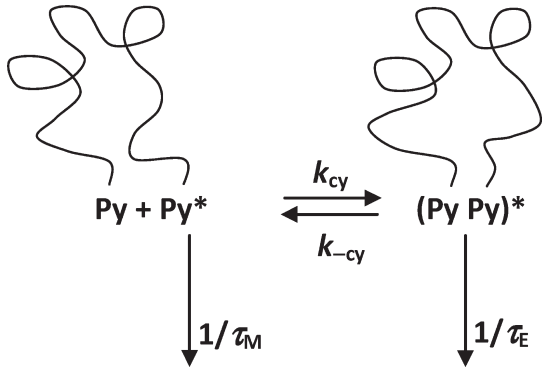

Scheme 4. End-to-End Cyclization According to the Fluorescence Blob Model

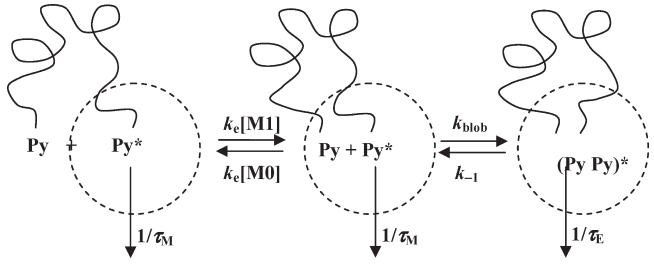

$$f_M(t) = \gamma \times \exp(-t/\tau_{M1}) + (1-\gamma) \times \exp(-t/\tau_M) \quad \text{with} \quad 0 < \gamma < 1 \quad (8)$$

$$f_E(t) = \exp(-t/\tau_E) \quad (9)$$

The functions $f_M(t)$ and $f_E(t)$ describe the natural decay of the pyrene monomer and excimer, respectively. $f_M(t)$ was found to depart from the monoexponential form typically expected for small molecules in solution certainly due to residual interactions between pyrene and the PEO backbone. A second decay time τ_{M1} was introduced in eq 8. The main difference between eq 1 obtained with Birks' scheme and eq 3 obtained from the FBM resides in the definition of f_{Mfree}. In the case of Birks' scheme, f_{Mfree} represents the fraction of pyrenes that do not form excimer resulting from PEO chains labeled at one end only. Consequently, f_{Mfree} describes the labeled PEO sample and should not be affected by the viscosity of the solvent or τ_M. In the case of the FBM, f_{Mfree} represents the fraction of chains where the ground-state pyrene is so far from the excited pyrene that it cannot form excimer. As a result, any effect that facilitates the search of the polymer coil by the excited pyrene located at the chain end, such as a lower solvent viscosity, a shorter chain, or a longer monomer lifetime τ_M, is expected to result in a smaller f_{Mfree} fraction.

If the pyrene monomer decays exponentially, eqs 3 and 4 based on the FBM are both sums of four exponentials. Equations 1 and 2 based on Birks' scheme are sums of four and three exponentials, respectively. The kinetic parameters used in the FBM are k_{blob}, $k_e[M1]$, $k_e[M0]$, and τ_E, whereas Birks' scheme uses the parameters k_{cy}, k_{-cy}, and τ_E, implying that the FBM uses

one additional parameter. Here, however, we fix τ_E in the FBM analysis. Consequently, global analysis of the monomer and excimer fluorescence decays with the sets of eqs 1 and 2, and 3 and 4 with τ_E fixed, uses the same number of adjustable parameters.

EXPERIMENTAL SECTION

Materials. Distilled in glass *N*,*N*-dimethylformamide (DMF), tetrahydrofuran (THF), acetone, dioxane, and HPLC grade methanol (MeOH) were purchased from Caledon Laboratories (Georgetown, ON). HPLC grade acetonitrile (ACN) and ethanol (EtOH) were obtained from Fischer Scientific (FairLawn, NJ). EMD Science (Gibbstown, NJ) and Sigma-Aldrich (Oakville, ON) supplied HPLC grade toluene and *N*,*N*-dimethylacetamide (DMA), respectively. All solvents were used as received. The poly(ethylene oxide) (M_n = 2K, 5K, 10K, and 16.5K) and poly(ethylene oxide) methyl ether (M_n = 2K) samples were purchased from Polymer Source (Montreal, QC). 1-Pyrenemethanol (98%) and 1-methylpyrene (97%) were purchased from Aldrich.

Synthesis of the Mono- and Doubly-Labeled PEO. The synthesis of the PEO(2K)−Py sample is described in the Supporting Information. The same synthesis procedure was used to prepare all PEO(X)−Py_2 samples. The structure of PEO(X)−Py_2 is shown in Figure 1. The yield of the labeling reaction determined by UV−vis absorption measurements was greater than 94% ensuring that most chain ends were capped by a pyrenyl pendant.

The number-average molecular weight, polydispersity index (PDI), and pyrene content of the pyrene-labeled PEO samples are given in Table 1.

Synthesis of 1-Pyrenemethyl Methyl Ether ($PyCH_2OMe$). Synthesis of $PyCH_2OMe$ was carried out according to Scheme 5. A detailed description of the synthesis is given in the Supporting Information.

Absorption Measurements. Absorption spectra were acquired on a Cary 100 UV−vis spectrophotometer with a UV cell having a 1 cm path length.

Pyrene Content Determination. The pyrene content (λ_{Py}) of the labeled PEOs was determined by measuring the absorption (Abs) of a DMF solution of known mass concentration of the labeled polymer [Poly] expressed in $g \cdot L^{-1}$. The pyrene content was obtained directly from the quantity Abs/([Poly] × ε_{Py}), where ε_{Py} is the molar absorption coefficient of 1-pyrenemethanol in DMF (ε_{Py} = 38 900 $M^{-1} \cdot cm^{-1}$ at 344 nm). We note that the molar absorption coefficient of 1-pyrenemethanol is the same as that of $PyCH_2OMe$ in DMF (ε_{Py} = 39 000 $M^{-1} \cdot cm^{-1}$ at 344 nm).

Intrinsic Viscosity Measurements. The intrinsic viscosity of the PEO sample with a molecular weight of 10 000 $g \cdot mol^{-1}$ was determined in the seven organic solvents used in the fluorescence experiments. An Ubbelohde viscometer was used with a water bath to maintain the temperature at 25 ± 0.1 °C. Four polymer concentrations ranging from 4.5 to 10 $g \cdot L^{-1}$ were used to obtain the intrinsic viscosity in each solvent. Plotting the reduced viscosity of the polymer solution as a function of polymer concentration yielded a straight line whose intercept was taken as the intrinsic viscosity [η].

Steady-State Fluorescence Measurements. The steady-state fluorescence spectra were acquired on a PTI fluorometer equipped with an Ushio UXL-75Xe xenon arc lamp and PTI 814 photomultiplier detection system. All spectra were acquired with the right angle geometry. After degassing for 30 min under a gentle flow of N_2 to remove oxygen, the solutions were excited at a wavelength of 344 nm, and the emission spectrum was acquired from 350 to 600 nm. For each PEO(X)−Py_2 sample, the fluorescence intensity of the monomer (I_M) was calculated by integrating the fluorescence spectrum from 372 to 378 nm. The fluorescence intensity of the excimer (I_E) was determined by normalizing the fluorescence spectrum of the monolabeled PEO(2K)−Py sample to that of PEO(X)−Py_2 at the first monomer peak (~375 nm), subtracting the normalized spectrum of PEO(2K)−Py from that of PEO(X)−Py_2, and integrating the result of that subtraction from 500 to 530 nm. This procedure ensured that no residual monomer fluorescence that might have leaked into the excimer emission would contribute to the calculation of the I_E/I_M ratio.

Time-Resolved Fluorescence Measurements. All polymer solutions for time-resolved fluorescence measurements were prepared following the same protocol as for the steady-state fluorescence experiments. The instrumentation used in the

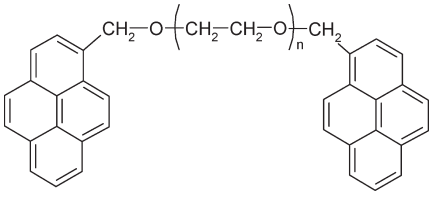

Figure 1. Chemical structures of the PEO(X)−Py_2 samples.

Scheme 5. Synthesis of 1-Pyrenemethyl Methyl Ether

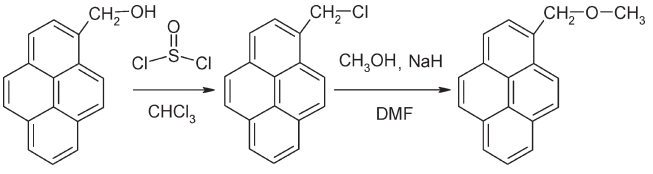

Table 1. PEO Molecular Weights, PDI, Pyrene Contents λ_{Py} in μmol/g Polymer, and the Labeling Efficiency for the PEO(2K)−Py and PEO(X)−Py_2 Samples

sample	M_n (PEO)[a] (g/mol)	PDI[a]	λ_{Py}[b] (μmol/g)	no. of labeled ends[c] (no. of ends)
PEO(2K)−Py	2000	1.05	446	0.99 (1)
PEO(2K)−Py_2	2000	1.10	800	1.93 (2)
PEO(5K)−Py_2	5000	1.08	350	1.89 (2)
PEO(10K)−Py_2	10000	1.05	184	1.92 (2)
PEO(16.5K)−Py_2	16500	1.05	113	1.91 (2)

[a] Information supplied by Polymer Source. [b] Measured by UV−vis absorption. [c] Number of labeled ends = $\lambda_{Py} \times M_n/(1 - \lambda_{Py} \times M_{Py})$, where M_{Py} = 215 $g \cdot mol^{-1}$ for pyrene−CH_2−.

dx.doi.org/10.1021/jp109528h |*J. Phys. Chem. B* 2011, 115, 3289–3302

time-resolved fluorescence measurements has been described earlier.[31]

Analysis of the Fluorescence Decays. The analysis of the monomer and excimer decays was done globally using, respectively, eqs 1 and 2 for Birks' scheme and eqs 3 and 4 for the FBM. The two sets of equations were convoluted with the instrument response function. The parameters were optimized using the Marquardt−Levenberg algorithm to obtain the best χ^2.[42] A light scattering correction was applied to the analysis of the fluorescence decays to account for the presence of residual light scattering. An additional parameter was added to account for the background noise that became somewhat important when studying PEO(X)−Py_2 constructs prepared with the longer PEO chains or in high viscosity solvents. The fits were considered good when the χ^2 was less than 1.30, and the residuals and autocorrelation of the residuals were randomly distributed around zero.

A special note must be made that, in these global analyses of the pyrene monomer and excimer fluorescence decays, the parameters k_{cy}, k_{-cy}, and τ_E for eqs 1 and 2 were fitted directly. Similarly, k_{blob}, $k_e[M0]$, $k_e[M1]$, and τ_E in eqs 3 and 4 were fitted directly. This represents a departure from the usual analysis of fluorescence decays with a sum of exponentials where the various rate constants describing the kinetics of excimer formation are derived from the decay times and pre-exponential factors retrieved from the analysis. Directly fitting the parameters gives control to the experimentalist on whether a given parameter should be allowed to float or be fixed.

Determination of the Natural Lifetime τ_M of the Pyrene Label. τ_M was estimated by comparing the lifetime of several pyrene derivatives, namely, the lifetime of 1-methylpyrene (PyMe), 1-pyrenemethanol ($PyCH_2OH$), 1-pyrenemethyl methyl ether ($PyCH_2OMe$), and PEO(2K)−Py in several organic solvents. The lifetimes of the pyrene derivatives are reported in Table SI.1. PEO(2K)−Py yields slightly biexponential decays with more than 92% of the pre-exponential weight obtained for the long decaytime τ_{M2} which was attributed to τ_M. The existence of a second decay time for PEO(2K)−Py is attributed to interactions taking place between the polymer backbone and the pyrene label. Comparison of the τ_M values obtained for PEO(2K)−Py and the lifetime of $PyCH_2OMe$ shows that within experimental error, these values are identical, differing by less than 1.0%. On the other hand, the lifetimes of $PyCH_2OH$ and PyMe are, on average, 7% and 30% smaller than τ_M, respectively. Except for the lifetime obtained in THF, a good agreement is observed between the τ_M values found in this work for PyMe and those reported by others in a recent publication.[30] However, the different τ_M values found for $PyCH_2OH$ and PyMe with respect to PEO(2K)−Py suggest that these two pyrene derivatives are not appropriate model compounds to estimate τ_M for the PEO(X)−Py_2 samples.

RESULTS AND DISCUSSION

All pyrene labeled PEO samples were studied in seven organic solvents that were chosen to cover a range of viscosities from 0.32 to 1.92 mPa·s while maintaining a similar solvent quality toward PEO. The solvent quality toward PEO was estimated by measuring the intrinsic viscosity of a monodisperse PEO sample (M_n = 10 000; PDI = 1.05) in the seven organic solvents listed in Table SI.2. The intrinsic viscosity did not depend much on solvent, taking an average value of 22.1 ± 0.4 mL·g^{-1}. These values are quite reasonable when compared to those reported earlier for a similar PEO sample (M_n = 9600; PDI = 1.10) in tetrahydrofuran, toluene, *N*,*N*-dimethylformamide, and dioxane and found to equal 21.7 ± 0.8 mL·g^{-1}.[21] The similar intrinsic viscosity values obtained for PEO in seven different organic solvents suggests that the PEO chain adopts similar dimensions in terms of end-to-end distance or radius of gyration in these different solvents.

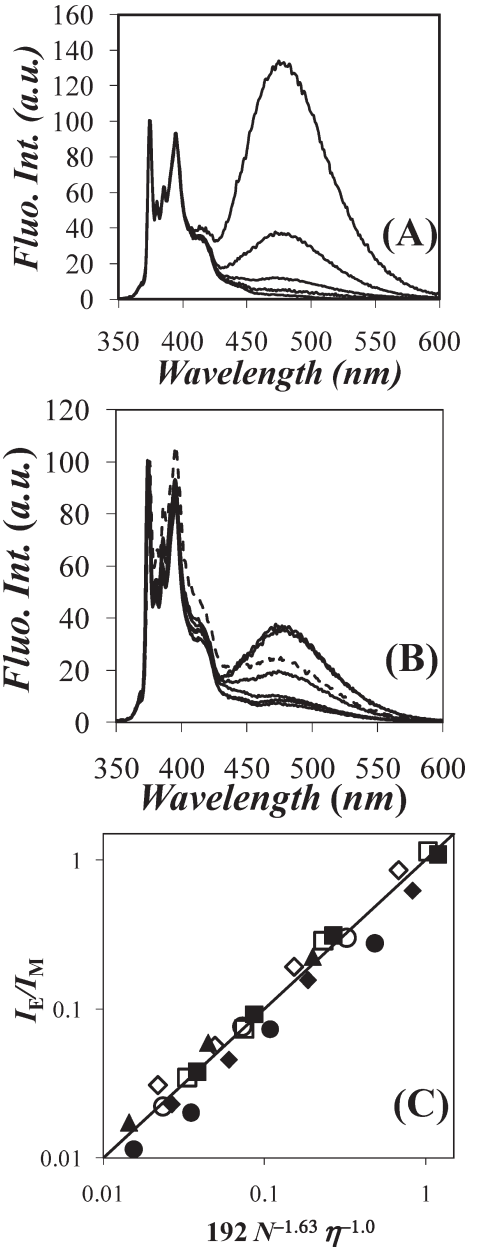

Figure 2. Steady-state fluorescence spectra of PEO labeled with pyrene (A) PEO(X)−Py_2 and PEO(2K)−Py in acetone with, from top to bottom, X = 2.0, 5.0, 10.0, 16.5, PEO(2K)−Py; (B) PEO(5K)−Py_2, from top to bottom, acetone (η = 0.32 mPa·s), ACN (η = 0.37 mPa·s), THF (η = 0.46 mPa·s), toluene (η = 0.56 mPa·s), DMF (η = 0.79 mPa·s), dioxane (η = 1.18 mPa·s), DMA (η = 1.92 mPa·s). (C) Scaling relationship for the I_E/I_M ratio with viscosity and chain length for (■) acetone, (□) ACN, (♦) THF, (◊) toluene, (●) DMF, (○) dioxane, (▲) DMA. [Py] = 2.5 × 10^{-6} M, λ_{ex} = 344 nm.

Analysis of the Steady-State Fluorescence Spectra. The steady-state fluorescence spectra of the PEO(X)−Py_2 and

dx.doi.org/10.1021/jp109528h |*J. Phys. Chem. B* 2011, 115, 3289–3302

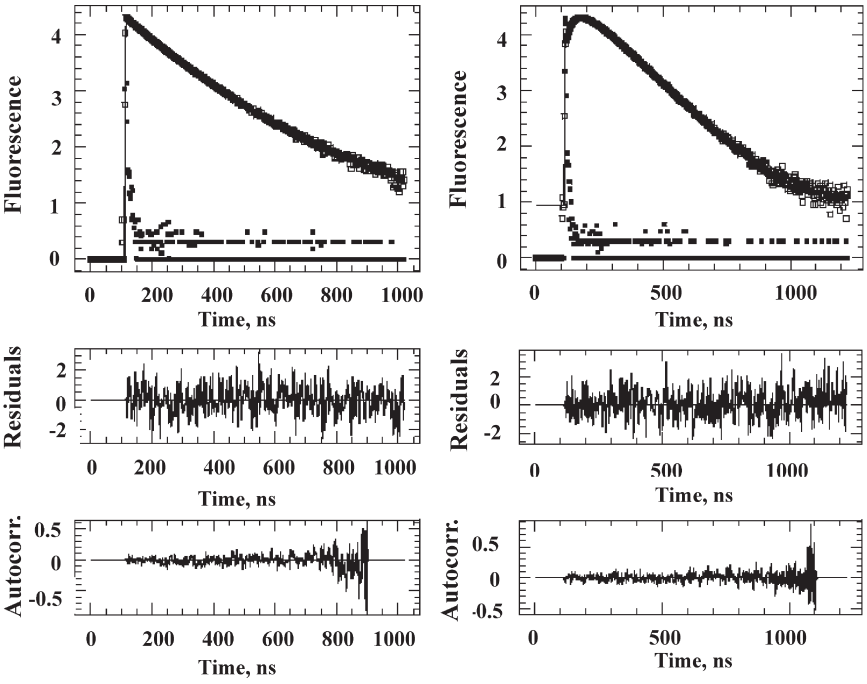

Figure 3. Fluorescence decays fitted by Birks' scheme of the pyrene monomer (left: λ_{ex} = 344 nm, λ_{em} = 375 nm; TPC = 2.04 ns/ch) and excimer (right: λ_{ex} = 344 nm, λ_{em} = 510 nm; TPC = 2.04 ns/ch) of PEO(2K)−Py_2 in dioxane. [Py] = 2.5 × 10^{-6} M, χ^2 = 1.01.

PEO(2K)−Py samples were acquired with a pyrene concentration of 2.5 × 10^{-6} M in the same organic solvents as those used in Table SI.2. The fluorescence spectra were also acquired with a concentration of 1.2 × 10^{-6} M. The excellent overlap observed for the fluorescence spectra obtained at the two concentrations ensured that the solutions were dilute enough for excimer formation to occur intramolecularly. The fluorescence spectra normalized at 375 nm of the PEO(X)−Py_2 series in acetone are shown in Figure 2A. As the PEO chain length increases, the emission at 480 nm typical of the excimer decreases, reflecting the decrease in the number of EEC events. A viscous solvent also hinders excimer formation as can be seen in Figure 2B where excimer fluorescence decreases strongly with increasing solvent viscosity. Some changes are observed in the features of the monomer fluorescence where the intensity of the third peak increases with respect to the intensity of the first peak as the solvent becomes less polar. The effect is particularly obvious in toluene, which is the least polar solvent used in this study (see dashed trace in Figure 2B). This effect reflects the sensitivity of the first peak located at ∼375 nm in the fluorescence spectrum to solvent polarity and is the result of a symmetry-forbidden transition.[43−47] Although the substitution of pyrene in the 1-position by a methyl or longer alkyl chain breaks the symmetry of pyrene, lowers the solvent sensitivity of the I_1/I_3 ratio, and shortens the unquenched fluorescence lifetime of the pyrene derivative, introduction of a β-oxygen in an alkyl pyrene substituent at the 1-position (as in 1-alkoxymethylpyrene) helps to resymmetrize the pyrene molecular orbitals.[48] As a consequence, the solvent sensitivity of the I_1/I_3 ratio is amplified and the lifetime is longer compared to that of 1-alkylpyrenes (see Table SI.1).

Since the first peak is typically taken to represent the monomer fluorescence intensity, the sensitivity of the symmetry-forbidden transition to solvent polarity suggests that care must be applied when using the pyrene fluorescence spectra to compare the process of excimer formation in different solvents. Nevertheless, Figure 2B indicates that the monomer fluorescence spectra overlap relatively well in all solvents except toluene so that if this effect plays a part, it will at most affect the results obtained in toluene only. The reduction in excimer formation with increasing polymer chain length and solvent viscosity observed in Figures 2A and 2B was summarized by determining the ratio of the fluorescence intensity of the excimer over that of the monomer, namely, the I_E/I_M ratio. The I_E/I_M ratio was calculated for all PEO(X)−Py_2 samples in all solvents and is plotted in Figure 2C where it was found to scale as $\eta^{-1.0} \times N_n^{-1.6}$. Despite the possible effect of solvent polarity on the I_E/I_M ratio, the scaling relationship found for the I_E/I_M ratio in Figure 2C is in excellent agreement with what is theoretically expected[33] and experimentally found[13−21,35] as shown hereafter.

The steady-state fluorescence spectra shown in Figures 2A and 2B differ from those reported[30] for a 9500 g·mol^{-1} PEO end-labeled with a 1-pyrenemethylene oxide derivative (PEO(9.5K)−Py_2) having supposedly the same chemical structure as the PEO(X)−Py_2 samples prepared for the present study. In particular, the features of the pyrene monomer fluorescence of PEO(9.5K)−Py_2 were quite different from those shown in Figure 2B, but similar to those expected of a 1-pyrenebutyl derivative (see fluorescence spectra given in refs 17, 21, 24−29, 31, and 49). This leads us to suspect that the PEO(9.5K)−Py_2 sample described in ref 30 was labeled with a 1-pyrenebutyl derivative. Since a 1-pyrenebutyl derivative in organic solvents has been shown to have a fluorescence lifetime that is about 70 ns shorter than that of a 1-pyrenemethyl derivative,[49] conclusions drawn in ref 30 from the analysis of the fluorescence decays acquired with PEO(9.5K)−Py_2 must be treated cautiously.

Cuniberti and Perico have suggested that at room temperature where the dissociation rate constant (k_{-cy}) is negligible, the I_E/I_M ratio is given by eq 10 and is proportional to k_{cy}, itself equal to $k_1 \times [Py]_{loc}$ where k_1 is the diffusion-controlled rate constant of

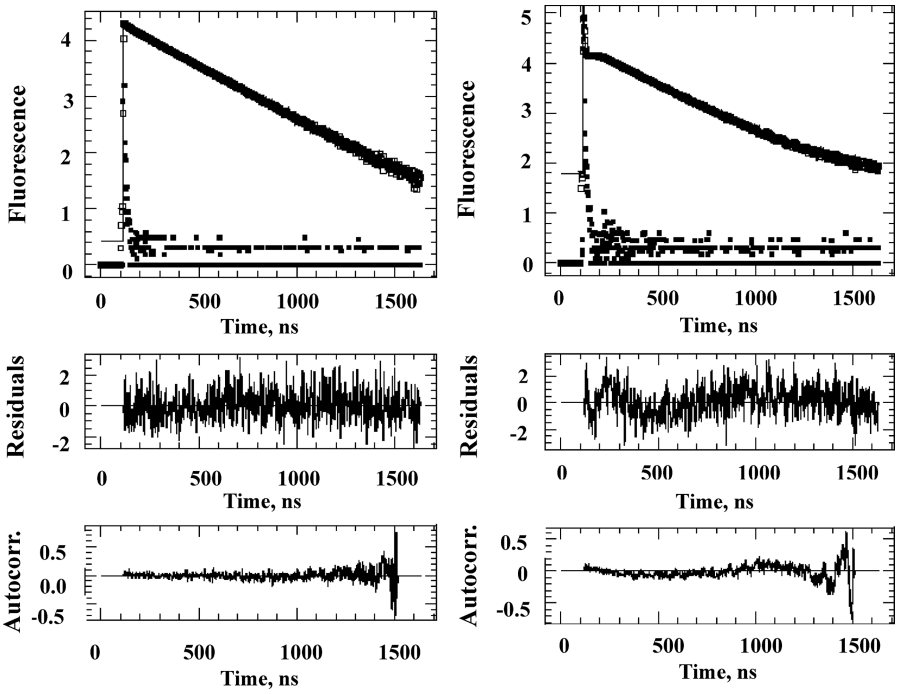

Figure 4. Fluorescence decays fitted by Birks' scheme of the pyrene monomer (left: λ_{ex} = 344 nm, λ_{em} = 375 nm; TPC = 2.04 ns/ch) and excimer (right: λ_{ex} = 344 nm, λ_{em} = 510 nm; TPC = 2.04 ns/ch) of PEO(10K)−Py_2 in dioxane. [Py] = 2.5 × 10^{-6} M, χ^2 = 1.19.

excimer formation and $[Py]_{loc}$ is the local concentration of pyrenes inside the polymer coil.[33]

$$\frac{I_E}{I_M} = \kappa \frac{\phi_E^o}{\phi_M^o} \tau_M k_1 [Py]_{loc} \qquad (10)$$

In eq 10, κ is a constant that depends on the geometry and sensitivity of the instrument used, ϕ_M^o and ϕ_E^o are the fluorescence quantum yields of the pyrene monomer and excimer, respectively, and τ_M is the lifetime of the pyrene monomer. The I_E/I_M ratio has been found to scale as $N^{-\alpha}$ for a number of pyrene end-labeled polymers and oligomers where α takes values ranging from 0.9 to 1.9.[13−20,35] Furthermore, k_1 representing a process controlled by diffusion is expected to be inversely proportional to viscosity,[21,33] as found experimentally in Figure 2C for the I_E/I_M ratio.

Analysis of the Fluorescence Decays According to Birks' Scheme. The excellent agreement observed between theory and experiment for the I_E/I_M ratio suggests that k_{cy} obtained directly from the analysis of the monomer and excimer fluorescence decays of the PEO(X)−Py_2 samples should obey a similar scaling relationship as the one obtained for the I_E/I_M ratio. To this end, the fluorescence decays of the pyrene monomer and excimer were acquired in all organic solvents. They were fitted globally with eqs 1 and 2. The pre-exponential factors and decay times retrieved from this analysis are listed in Table SI.3A. For the shorter chains and lower viscosity solvents, the fits were excellent with all χ^2 being smaller than 1.20, and the residuals and the autocorrelation of the residuals being randomly distributed around zero. A sample decay analysis is shown in Figure 3. The monomer and excimer decays are shown on the left and right side of the figure, respectively.

As the chain length was increased from 2K in Figure 3 to 10K in Figure 4, the quality of the fits became poorer, in particular for the excimer decay. Excimer formation is strongly reduced according to the $I_E/I_M \sim N^{-1.6}$ relationship found in Figure 2C, and the background level in the excimer decay is increased in Figure 4. The excimer decays for both PEO(2K)−Py_2 and PEO(10K)−Py_2 exhibit a rise time, but a spike appears at early times in the excimer decay of PEO(10K)−Py_2 only. This spike became prominent as excimer formation was reduced, either due to the use of a high viscosity solvent, a long PEO chain, or both. The existence of this fast decay has been reported previously and has been attributed to the presence of ground-state dimers.[29,30,39] Nevertheless, it must be acknowledged that in the present study, this spike occurred only when the excimer emission was weak, so that the possibility that it might be due to light scattering or the presence of an impurity, due to a possible postdegradation of pyrene, cannot be ruled out. To handle the spike, an additional exponential was added for the analysis of the monomer and excimer fluorescence decays with a decay time (τ_S) fixed to 3.5 ns as this value has been found in other studies[29,30,39] (see eqs 1 and 2, and 3 and 4).

The cyclization rate constant, k_{cy}, the dissociation rate constant, k_{-cy}, and the excimer lifetime, τ_E, were determined directly from the global analysis of the monomer and excimer fluorescence decays. Their values are reported in Table SI.3B. Since they were found to depend on viscosity (η) and the number average degree of polymerization (N_n), their scaling behavior was determined as a function of η and N_n as shown in Figures 5A−C. Equation 10 predicts that k_{cy} should scale as η^{-1} and $N_n^{-\alpha}$, where α values have been found to range from 0.9 to 1.9 experimentally.[13−20,35] For small N_n and η values, k_{cy} was found to scale as $\eta^{-1} \times N_n^{-1.34}$. Although an exponent of −1.34 is consistent with values reported in the literature, it is nevertheless different from that of −1.6 found for the I_E/I_M ratios in Figure 2C. Furthermore, for larger N_n and η values, k_{cy} in Figure 5A remained constant within experimental error. A similar break point was also observed in the trends for k_{-cy} and τ_E.

Since k_{-cy} and τ_E describe intrinsic properties of the excimer, they are not expected to vary with polymer length as long as the polymer is long enough. Interestingly, the opposite is observed

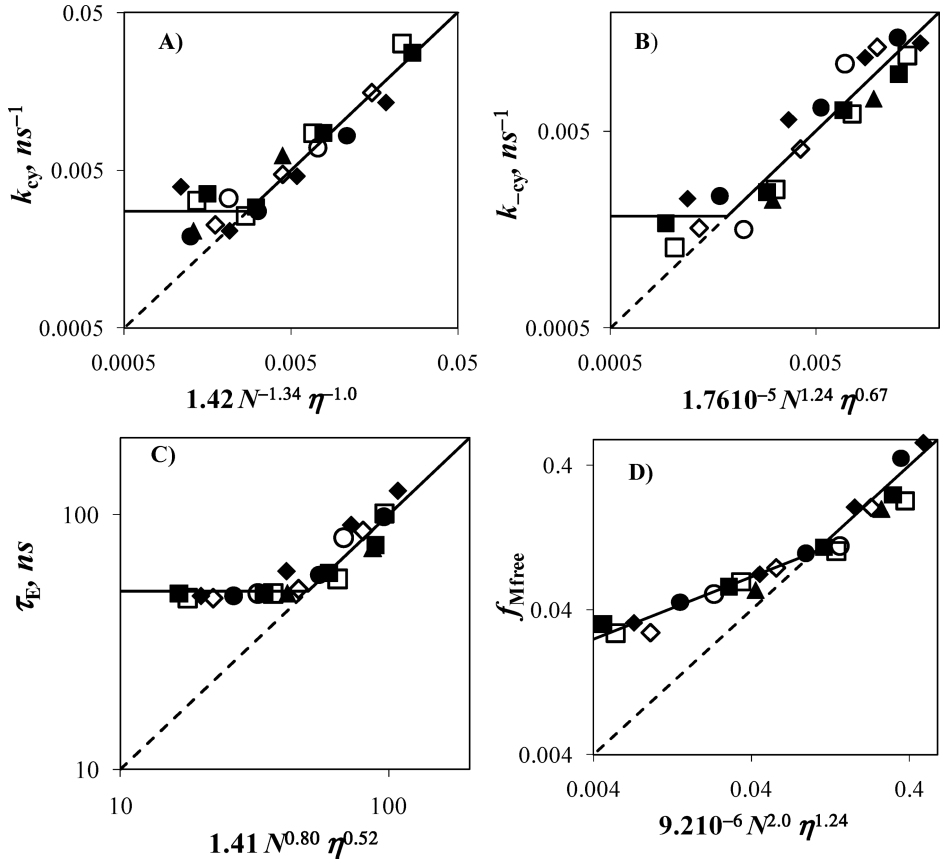

Figure 5. Scaling behavior of the parameters obtained from the global analysis of the pyrene monomer and excimer experimental fluorescence decays fitted with eqs 1 and 2, respectively. Symbols are the same as for Figure 2C.

where k_{-cy} and τ_E take constant values of, respectively, 1.8 ($\pm$0.5) $\times$ 10^6 s^{-1} and 48 $\pm$ 1 ns for small N_n and η values. These values for k_{-cy} and τ_E are quite reasonable for pyrene excimer in organic solvents[38] with k_{-cy} being about 10 times smaller than τ_E^{-1}, which supports the notion that the dissociation of the pyrene excimer is negligible at room temperature as was assumed to derive eq 10. However, k_{-cy} and τ_E were found to increase markedly for larger N_n and η values. Incidentally, this behavior was also observed for a series of pyrene end-labeled monodisperse polystyrenes.[31] As it turns out, all trends shown in Figures 5A−C show a break point that occurs for N_n and η values such that $N_n \times \eta \sim 80$ mPa·s.

Another parameter which was found to behave unexpectedly is the fraction f_{Mfree}, representing the molar fraction of pyrene monomers that do not form excimer and emit as if they were free in solution. f_{Mfree} equals $[Py^*_{free}]_o/([Py^*_{diff}]_o + [Py^*_{free}]_o)$ (see eq 1 for the definition of $[Py^*_{diff}]$ and $[Py^*_{free}]_o$) and is plotted as a function of viscosity in Figure 6. The fraction f_{Mfree} was never equal to zero as a small amount (less than 5 mol % of the PEO chains) of monolabeled polymer is always present in the samples. Interestingly, f_{Mfree} was found to increase linearly with increasing viscosity, and the increase was more pronounced with increasing polymer chain length. This result was unexpected, since f_{Mfree} is supposedly a measure of the labeling efficiency of the polymer, which depends on neither solvent nor polymer chain length. f_{Mfree} remained relatively small (i.e., < 0.1) for N_n and η values, such that $N_n \times \eta < 80$ mPa·s, but for larger N_n and η values, f_{Mfree} took much larger values as large as 0.85 in dioxane for PEO(10K)−Py_2. In the log−log plot presented in Figure 5D, a break point for f_{Mfree} can be observed for $N_n \times \eta > 80$ mPa·s. Recently, a similar increase in f_{Mfree} with increasing viscosity has been observed in our laboratory for a series of pyrene end-labeled monodisperse poly(*N*-isopropylacrylamide)s (PNIPAM) in mixtures of 1-hexanol and methanol used to modify the solvent viscosity without affecting its quality toward the PNIPAM backbone. This observation made with both PEO and PNIPAM pyrene end-labeled polymers suggests that the effect shown in Figure 6A might be general.

The trends shown in Figures 5A−D can be summarized as follows. As long as the chain is short and the solvent is fluid such that $N \times \eta < 80$ mPa·s, k_{cy} decreases with increasing chain length and viscosity as $\eta^{-1.0} \times N_n^{-1.34}$, k_{-cy} and τ_E remain constant, and f_{Mfree} is small. In other words, the parameters k_{cy}, k_{-cy}, τ_E, and f_{Mfree} behave as expected in this range of N and η values. For N and η values resulting in $N \times \eta$ being larger than 80 mPa·s, k_{cy} plateaus and k_{-cy}, τ_E, and f_{Mfree} increase with increasing viscosity and chain length. We have demonstrated in the Supporting Information that these discrepancies are due neither to limitations in the analysis of the fluorescence decays nor to the presence of fluorescent impurities whose emission might overlap that of the pyrene monomer and/or excimer. Consequently, our results suggest that Birks' scheme does not apply to study the EEC kinetics of long chains in viscous solvents and that an alternative analysis is required under such conditions.

Fluorescence Blob Model Analysis of the Fluorescence Decays. Excimer formation for PEO(10K)−Py_2 in dioxane represents a case in point for this study. Global analysis of the monomer and excimer decays with eqs 1 and 2 yields an f_{Mfree} value of ~0.85. Indeed the fluorescence decays of the pyrene monomer acquired for PEO(10K)−Py_2 and PEO(2K)−Py are

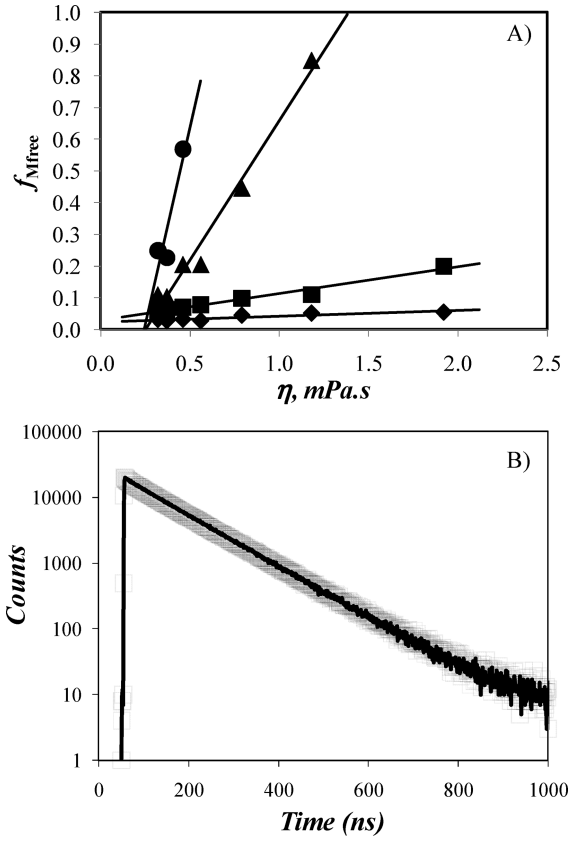

Figure 6. (A) Fraction f_{Mfree} obtained from the global analysis of the monomer and excimer fluorescence decays with eqs 1 and 2. (♦) PEO(2K)−Py_2, (■) PEO(5K)−Py_2, (▲) PEO(10K)−Py_2, and (●) PEO(16.5K)−Py_2. (B) Monomer fluorescence decays of (—) PEO(2K)−Py and (□) PEO(10K)−Py_2 in dioxane.

essentially superimposable in Figure 6B suggesting that no excimer forms. Yet, after the prominent spike found at the early times and characteristic of the Py_S^* species in eqs 1 and 2, a rise time is observed in the excimer decay of PEO(10K)−Py_2 in Figure 4, a clear indication that excimer formation occurs by diffusive encounters between the two ends. Together Figures 4 and 6B imply that a small fraction $(1 - f_{Mfree})$ of all excited pyrenes form excimer by diffusion. We postulate that those pyrenes that form excimer by diffusion are close to each other, closer than the overall distribution of end-to-end distances (r_{EE}) suggests. If this is the case, excimer formation for PEO(10K)−Py_2 in dioxane would involve only a small fraction $(1 - f_{Mfree})$ of all excited pyrenes, namely, those pyrene-labeled ends that are located within a distance r_{EE} smaller than a cutoff distance referred to as r_{EE}^{blob}. The superscript blob refers to the subvolume where excimer formation takes place inside the polymer coil.

Interestingly, the concept of localized reactivity inside the polymer coil can be easily handled by using the fluorescence blob model (FBM) which was originally developed to handle the complex kinetics of excimer formation encountered with polymers randomly labeled with pyrene.[40,41] According to the FBM, an excited pyrene probes a finite volume called a blob while it remains in the excited state. Excimer formation occurs inside a blob with a rate constant k_{blob}. Ground-state pyrenes can move inside the blob containing an excited pyrene with a rate constant k_e[M1], where k_e is the exchange rate constant and [M1] is the local concentration of blobs inside the polymer coil that contain one ground-state pyrene. Ground-state pyrenes exit the blob containing one excited pyrene with a rate constant k_e[M0], where [M0] is the local concentration of blobs that contain no ground-state pyrene. Application of the FBM to end-labeled polymers has been described in the Theory section, and eqs 3 and 4 were used to fit globally the monomer and excimer decays, respectively. All fits were excellent, even for PEO(X)−Py_2 samples prepared with long PEO chains and/or large solvent viscosity, yielding small χ^2 values (<1.20), randomly distributed residuals, and autocorrelation function of the residuals. The parameters retrieved from the fits are listed in Table SI.5. In particular, the poorer fits obtained for the Birks' scheme analysis of the fluorescence decays acquired with the longer chains in more viscous solvents are much improved as can be seen by comparing the fits shown in Figure 4 and Figure 7.

Figure 8 illustrates how k_{blob}, k_e[M1], k_e[M0], and f_{P1} (f_{P1} = [M1]/([M1] + [M0] + $[Py^*_{free}]_o$), the molar fraction of pyrenes located in a blob containing the excited pyrene and one ground-state pyrene, behave as a function of solvent viscosity and polymer molecular weight. As the viscosity increases or the molecular weight increases, k_{blob} in Figure 8A decreases. However, the data show substantial scatter for the PEO constructs with a high molecular weight and solutions with large solvent viscosities. The increased scatter found for k_{blob} reflects the fact that as chain length or solvent viscosity increases, the fraction of pyrenes forming excimer inside a blob decreases. This effect explains also why k_e[M1] decreases and k_e[M0] increases with increasing η and M_n in Figure 8B. As the size of the polymer coil expands with increasing M_n, the local concentration of blobs inside the polymer coil containing the ground-state pyrene ([M1]) decreases whereas [M0] increases. A similar effect is achieved by increasing the solvent viscosity.

As the solvent viscosity increases, the size of a blob decreases and [M1] decreases whereas [M0] increases. It is worth noting that M1 (the blobs that contain the ground-state pyrene) and M0 (the blobs that contain no ground-state pyrene) provide information about the behavior of the pyrenes that are involved in the process of excimer formation. As the chain length and solvent viscosity become too large, a substantial fraction of the excited pyrenes are unable to form excimer. These pyrenes are denoted by Py^*_{free} in eq 3, and their contribution increased with increasing η and M_n. When taken into account, one obtains the fractions of blobs that contain one ground-state pyrene f_{P1} (f_{P1} = [M1]/([M1] + [M0] + [Py_{free}])) which is given in Figure 8D. For short chains and low viscosity solvents, f_{P1} is close to 1.0, indicating that both chain ends are located inside the same blob. As M_n and η increase, the chance of finding both ends inside the same blob decreases to zero for the larger M_n and η values used in this study.

Based on this work, the analysis of the kinetics of excimer formation for pyrene end-labeled polymers yields distinct results for two different sets of sample and solvent conditions. The first set encompasses the PEO(X)−Py_2 samples prepared with short chains and low viscosity solvents. Here both pyrene-labeled ends are located in the same blob, and the rate constant of excimer formation k_{blob} is recovered with good accuracy and is found to decrease with increasing M_n and η. The second set involves samples with longer chains, where the fraction of blobs containing a ground-state pyrene (f_{P1} in Figure 8D) is much smaller. Since fewer pyrenes form excimer, k_{blob} is recovered with little accuracy, showing substantial scatter in Figure 8A, but seems to remain constant for large M_n and η values with several data points clustering around an average value of $k_{blob} = 1.5 \pm 0.3 \times 10^6$ s^{-1}.

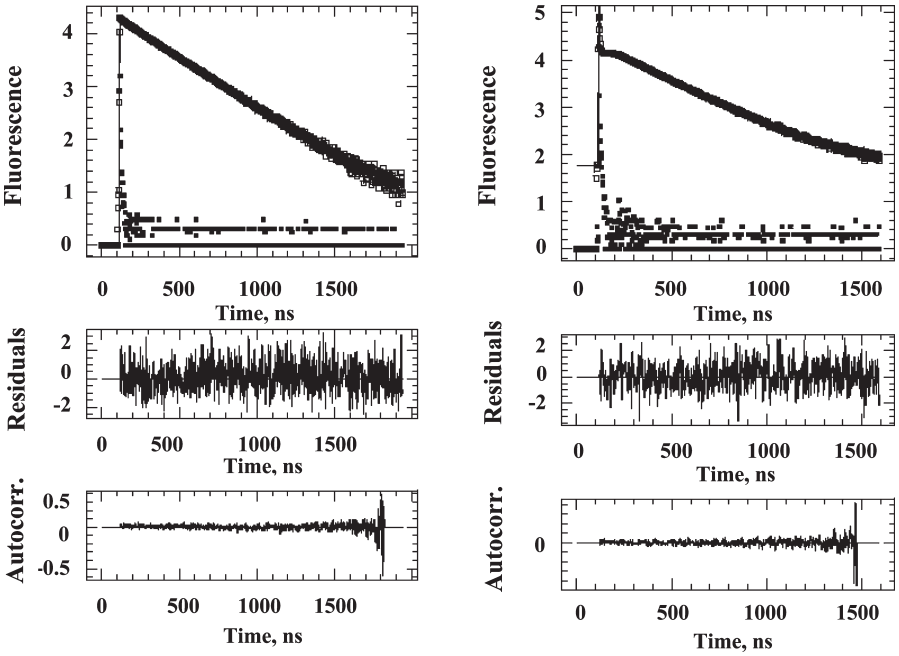

Figure 7. Fluorescence decays of the pyrene monomer (left: λ_{ex} = 344 nm, λ_{em} = 375 nm; TPC = 2.04 ns/ch) and excimer (right: λ_{ex} = 344 nm, λ_{em} = 510 nm; TPC = 2.04 ns/ch) of PEO(10K)−Py_2 in dioxane fitted with eqs 3 and 4, respectively. [Py] = 2.5 × 10^{-6} M, χ^2 = 1.06.

Comparison of the Steady-State and Time-Resolved Fluorescence Results. The above discussion implies that the kinetics of excimer formation for pyrene end-labeled polymers should fall into two regimes. The first regime encountered for short chains and low viscosity solvents describes excimer formation when both pyrene-labeled ends are located in the same blob. In effect, this regime is properly handled by Birks' scheme, as we have shown in Figure 5A−D. In this regime, k_{cy} scales as $N^{-1.34}$ in Figure 5A in agreement with earlier studies.[13−20,35] For longer chains and high viscosity solvents, a fraction of the pyrenes never meet, and these pyrenes do not form excimer. This second regime is not properly handled by Birks' scheme and is more realistically described by the FBM. It is, however, surprising that those two regimes so clearly identified by the time-resolved fluorescence measurements described in this study seem to go undetected by the steady-state fluorescence measurements shown in Figure 2C where no break-point between the two regimes is observed. An explanation for this apparent contradiction is provided below.

The above discussion suggests that excimer formation occurs inside a blob of radius r_{EE}^{blob} with an excimer rate constant k_{cy}^{blob} that remains the same regardless of polymer chain length, as long as the polymer chain length is such that the polymer coil radius is greater than r_{EE}^{blob}. The rate constants k_{-cy} and τ_E^{-1} are expected to retain the values obtained for shorter chains. Those PEO(10K)−Py_2 coils for which r_{EE} is larger than r_{EE}^{blob} do not form excimer and emit in the same manner as the pyrene monomer of PEO(2K)−Py. According to these conditions, the fraction f_{Mfree} of pyrene end groups that do not form excimer increases with increasing chain length or viscosity as observed experimentally in Figures 5D and 8D.

The concept of a blob discussed above is depicted in Scheme 6. It is applied to predict the scaling relationship that would exist between the I_E/I_M ratio and N_n. The mathematical derivation shown hereafter assumes that the coil is in a theta solvent and that the chain adopts a Gaussian conformation. According to Scheme 6, the experimentally found fraction of polymer coils (f_{P1}) whose pyrene-labeled ends are located inside a blob is given by the integral $\int_0^{Rblob}(\beta/\pi^{1/2})^{1/3}\ \exp(-\beta^2 r^2)4\pi r^2\ dr$, where $\beta^2 = 3/(2nl^2)$ with n and l being the number of Kuhn segments and Kuhn length, respectively. The I_E/I_M ratio is proportional to the ratio of the integrals $\int_0^\infty [E^*]_{(t)}\ dt/\int_0^\infty [M^*]_{(t)}\ dt$ which is given in eq 11 after integrating eqs 1 and 2. This derivation assumes that $f_{P1} = 1 - f_{Mfree}$ and neglects the contribution from the Py_S^* species whose lifetime τ_S equal to 3.5 ns is much shorter than the other decay times involved.

Implicit in the derivation of eq 11 is the fact that as N_n tends to infinity, k_{cy} tends to k_{cy}^{blob} and f_{Mfree} tends to unity. According to eq 11, the limit of $\int_0^\infty [E^*]_{(t)}\ dt/\int_0^\infty [M^*]_{(t)}\ dt$ when n becomes large equals a constant that does not depend on chain length multiplied by $n^{-1.5}$.

$$\frac{\int_0^\infty [E^*]_{(t)}\ dt}{\int_0^\infty [M^*]_{(t)}\ dt} \frac{\dfrac{k_{cy}(\tau_2-\tau_1)}{\sqrt{(X-Y)^2+4k_{cy}k_{-cy}}} \times (1-f_{Mfree})}{\dfrac{(X-\tau_2^{-1})\tau_1-(X-\tau_1^{-1})\tau_2}{\sqrt{(X-Y)^2+4k_{cy}k_{-cy}}} \times (1-f_{Mfree}) + f_{Mfree} \times \tau_M}$$

$$\xrightarrow[f_{Mfree}\to 1]{} \frac{1}{\tau_M} \frac{k_{cy}^{blob} \times (\tau_2-\tau_1)}{\sqrt{(X-Y)^2+4k_{cy}k_{-cy}}} \times (1-f_{Mfree}) \xrightarrow[n\to\infty]{}$$

$$\frac{1}{\tau_M} \frac{k_{cy}^{blob} \times (\tau_2-\tau_1)}{\sqrt{(X-Y)^2+4k_{cy}k_{-cy}}} \times \sqrt{\frac{6}{\pi}} \left(\frac{R_{blob}}{l}\right)^3 n^{-3/2} \qquad (11)$$

Furthermore, $k_{cy}^{blob} \times R_{blob}^3$ is expected to be inversely proportional to viscosity. Since the I_E/I_M ratio is proportional to $\int_0^\infty [E^*]_{(t)}\ dt/\int_0^\infty [M^*]_{(t)}\ dt$, eq 11 implies that the I_E/I_M ratio scales as $n^{-1.5} \times \eta^{-1}$ for longer chains, a scaling behavior similar to that expected for shorter chains where eq 10 holds. In other words, the I_E/I_M ratio is not expected to sense the switch that might be occurring when the chain becomes so large that a large fraction of the chain ends are no longer inside the blob. Only time-resolved fluorescence experiments can probe the switch depicted in Scheme 6, since these experiments yield the actual rate constants describing the process of EEC as

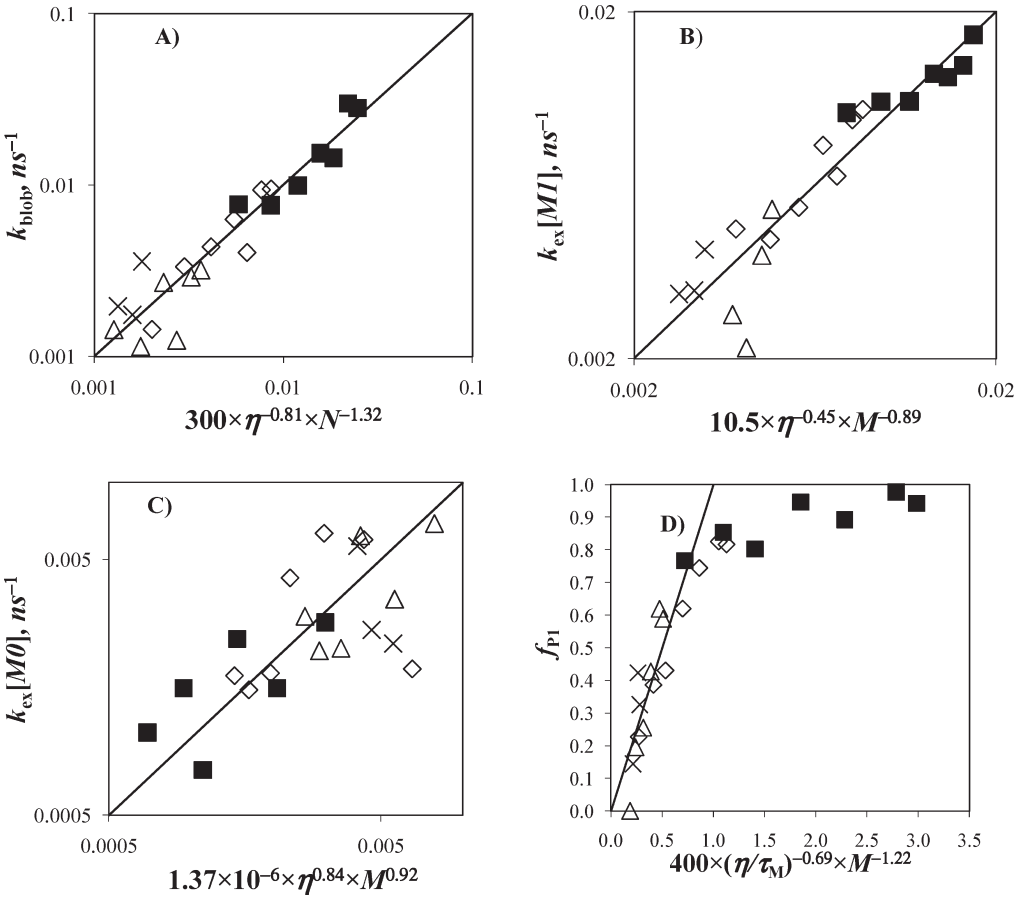

Figure 8. Scaling behavior of the parameters obtained from the global analysis of the pyrene monomer and excimer fluorescence decays of the Py−PEO(X) samples fitted with eqs 3 and 4, respectively. (■) PEO(2K)-Py_2, (◇) PEO(5K)-Py_2, (△) PEO(10K)-Py_2, (×) PEO(14.5K)-Py_2.

well as the fraction f_{P1} of excited chromophores involved in EEC events.

Information about the Distribution of End-to-End Distances. According to the FBM analysis of the fluorescence decays, the fraction f_{P1} represents the fraction of the chains whose ends are located in the same blob and close enough to form excimer. Consequently, f_{P1} is the probability of having the two polymer ends at a distance smaller than R_{blob}, and an expression of f_{P1} can be determined by using the Gaussian distribution of end-to-end distances. Its expression is given by eq 12 where the integral in the denominator equals unity.

$$f_{P1} = \frac{\int_0^{R_{blob}} \left(\frac{\beta}{\sqrt{\pi}}\right)^3 \exp(-\beta^2 r_{EE}^2) 4\pi r_{EE}^2 \, dr_{EE}}{\int_0^{\infty} \left(\frac{\beta}{\sqrt{\pi}}\right)^3 \exp(-\beta^2 r_{EE}^2) 4\pi r_{EE}^2 \, dr_{EE}} \qquad (12)$$

Equation 13 has been derived for the end-to-end distance (r_{EE}) of PEO in water.[50]

$$r_{EE} = 0.119 \times \sqrt{M_n} \times 0.707 \text{ nm} \qquad (13)$$

If the coil dimensions of the short PEO chains in the organic solvents used in this study are similar to that of PEO in water, eq 13 could also be used to determine r_{EE} of PEO in the organic solvents listed in Table SI.2. To establish whether this was the case, intrinsic viscosity ($[\eta]$) measurements were conducted for PEO(10K) in the seven organic solvents used in this study. $[\eta]$ was found to remain constant and equal to 22.1 ± 0.4 mL·g^{-1} (Table SI.2). This $[\eta]$ value happens to be close to that of PEO(10K) in water at 25 °C (23.9 mL·g^{-1}) estimated from the Mark−Houwink−Sakurada parameters $K = 49.9 \times 10^{-3}$ mL·g^{-1} and $a = 0.67$.[51] Comparison of the $[\eta]$ values obtained in water and DMF by using the relationship $[\eta] = 2.0 + 24.0 \times 10^{-3} \times M_n^{0.73}$ for PEO in DMF at 25 °C[51] indicates that the difference in $[\eta]$ between PEO in water and DMF differs by less than 8.2% for M_n values between 2 and 16 K, i.e., the range of M_n values used for the PEO(X)−Py_2 samples.

The effect that the pyrene label might have on the coil dimensions of the PEO(X)−Py_2 samples was investigated by measuring $[\eta]$ of PEO(5K)−Py_2 in DMF and comparing the $[\eta]$ value obtained for PEO(5K)−Py_2 with that of PEO(5K). Within experimental error, the $[\eta]$ value obtained for PEO(5K)−Py_2 in DMF (14.0 ± 0.2 mL·g^{-1}) matches that obtained for the unlabeled sample (14.0 ± 0.2 mL·g^{-1}). The results of these control experiments led us to the conclusion that the polymer coils of the PEO(X)−Py_2 samples must have similar dimensions in the organic solvents listed in Table SI.2 and water so that eq 13 could be used to estimate the r_{EE} values of the PEO(X)−Py_2 samples in these organic solvents.

Using the f_{P1} values reported in Figure 8D and eq 13 to estimate r_{EE} for the PEO(X)−Py_2 samples, eq 12 could be solved numerically to retrieve R_{blob}. Since the f_{P1} values reported in Figure 8D for PEO(2K)−Py_2 are close to unity, the FBM does

Scheme 6. Dependency of f_{Mfree} as a Function of r_{EE}/R_{blob}. Left: $r_{EE}/R_{blob} \ll 1$ and $f_{Mfree} = 0$. Right: $r_{EE}/R_{blob} > 1$ and $f_{Mfree} > 0$

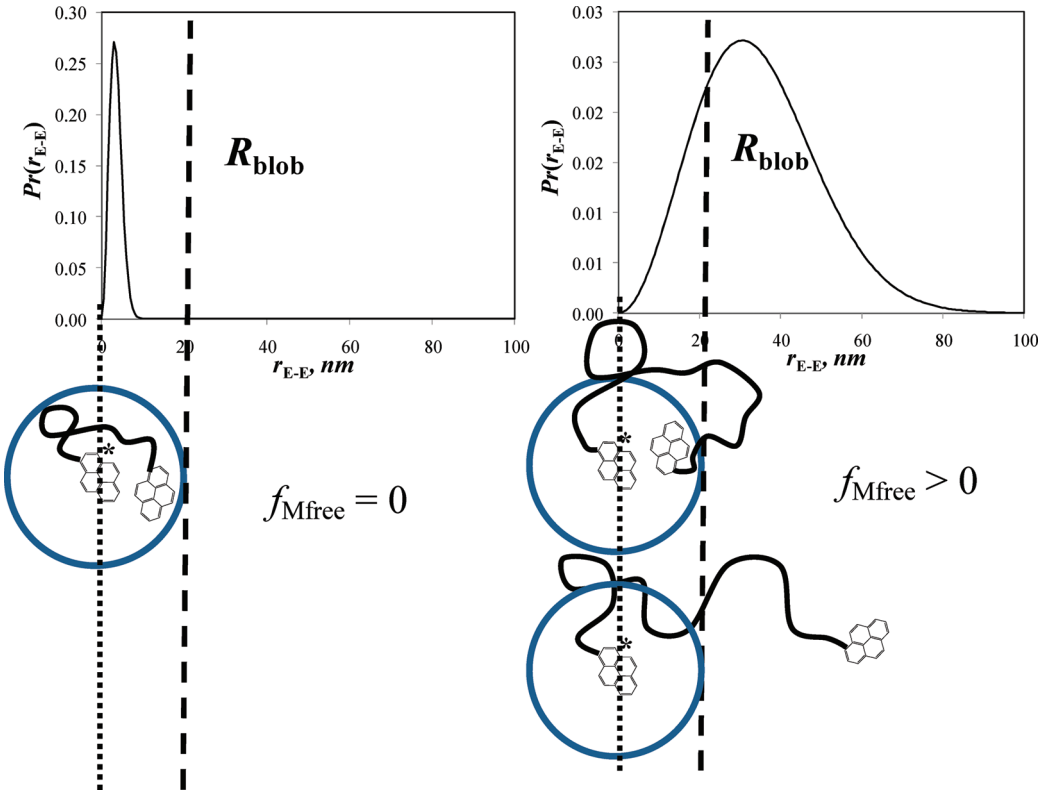

not apply for this sample. Consequently, R_{blob} was determined for the other PEO(X)−Py_2 samples, and it is plotted as a function of $(\tau_M/\eta)^{1/2}$ in Figure 9. Within experimental error, R_{blob} is found to increase linearly with increasing $(\tau_M/\eta)^{1/2}$. Since R_{blob} is expected to be a measure of the distance traveled by an excited pyrene undergoing Brownian motion, R_{blob} is expected to increase with increasing lifetime and decrease with increasing solvent viscosity as experimentally found in Figure 9. To the best of our knowledge, Figure 9 represents the first example in the literature where pyrene end-labeled monodisperse polymers have been used to retrieve information on the end-to-end distance distribution of polymers in solution.

CONCLUSIONS

A series of PEO(X)−Py_2 samples were synthesized, and their monomer and excimer fluorescence decays were acquired in seven organic solvents of viscosity ranging from 0.32 to 1.92 mPa·s. Analysis of the steady-state fluorescence spectra showed that the I_E/I_M ratio scaled as $\eta^{-1.0} \times N_n^{-1.6}$ as theory[33] and other experimental studies predict.[13−21,35] However, analysis of the fluorescence decays with Birks' scheme showed a major inconsistency. As polymer chain length and/or solvent viscosity were increased, an increasing fraction of excited pyrenes failed to form excimer. Refinement in the analysis programs coupled with simulations demonstrated that this effect is real. This effect was attributed to the fact that excimer formation occurs in a subvolume of the polymer coil. Analysis of the fluorescence decays with the FBM yielded a set of parameters which was internally consistent with the assumptions of the FBM.

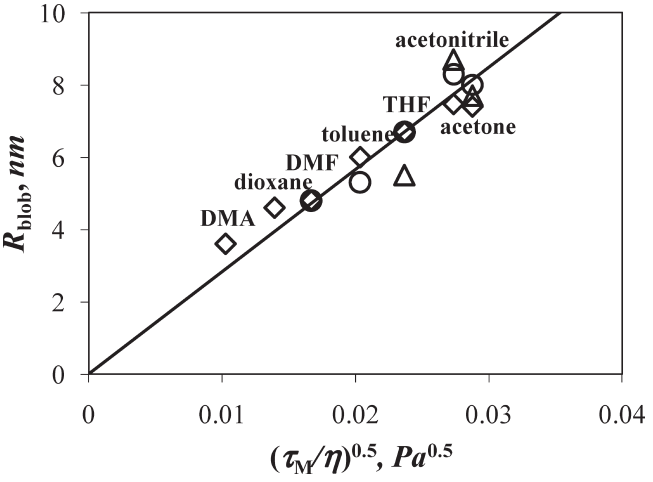

Figure 9. R_{blob} versus $(\tau_M/\eta)^{1/2}$ for PEO(5K)−Py_2 (◊), PEO(10K)−Py_2 (○), and PEO(16.5K)−Py_2 (△) in the following solvents (from left to right): DMA, dioxane, DMF, toluene, THF, acetonitrile, and acetone.

EEC of pyrene end-labeled monodisperse polymers has been thoroughly studied over the past three decades.[2−37] It is thus somewhat surprising that the inconsistencies uncovered in this report have been so far unnoticed. One reason for this resides in the nature of the label used to prepared pyrene end-labeled polymers. In many instances, a 1-pyrenebutyl derivative has been used.[17−21,23−29,31] This end group has a lifetime (τ_M) that is about 70 ns shorter than the 1-pyrenemethyl derivative used in this study.[49] The longer butyl linker provides enough flexibility

to ensure rapid rearrangement of the chain ends of a rigid polymer. For instance, some of us found out that EEC kinetics according to Birks' scheme were not followed when 1-pyrenemethylamine was used to label a series of monodisperse polystyrenes whereas they were when using 1-pyrenebutylamine.[31] The slow chain end rearrangements experienced with polystyrene that required the use of 1-pyrenebutylamine instead of 1-pyrenemethylamine was not a problem with the more flexible PEO backbone. As M_n and η increase, the long decay time τ_2 in eq 1 increases, and if τ_M is too short such as for the 1-pyrenebutyl derivative, τ_2 matches τ_M before the polymer coil is large enough for the two pyrene-labeled ends to be located in different blobs. Using a longer-lived pyrene label such as the 1-pyrenemethylene derivative employed in the present study enables one to probe the crossover between the two regimes. We suspect that this effect will require revisiting some of the conclusions which have been reached earlier for pyrene end-labeled polymers. In particular and if more experiments confirm the claims made in the present study, the assumption that the I_E/I_M ratio be readily taken as a sole measure of the rate constant of EEC[33] might no longer be valid as it also accounts for those pyrenes that cannot form excimer. Most importantly, and since Birks' scheme and the Wilemski−Fixman theoretical framework seem to be better suited to the study of pyrene end-labeled short chains or oligomers, these experiments will establish the universality of the FBM to study the chain dynamics of actual polymers by monitoring the encounters between a fluorophore and a quencher covalently attached to a polymer regardless of their position on the chain be they randomly distributed along the chain[31,40,41,49] or at the chain ends (cf. this work) when the polymer coil is larger than the volume of a blob.

■ ASSOCIATED CONTENT

Supporting Information. Derivation equations, tables of sample characteristics, and syntheses of samples. This material is available free of charge via the Internet at http://pubs.acs.org.

■ ACKNOWLEDGMENT

The authors are indebted for generous funding from NSERC and the Petroleum Research Fund. S.C. thanks Dr. Howard Siu for helpful discussions.

■ REFERENCES

(1) Jacobson, H.; Stockmayer, W. H. *J. Chem. Phys.* **1950**, *18*, 1600–1607 doi: 10.1063/1.1747547.
(2) Wilemski, G.; Fixman, M. *J. Chem. Phys.* **1974**, *60*, 866–877.
(3) Wilemski, G.; Fixman, M. *J. Chem. Phys.* **1974**, *60*, 878–890.
(4) Eaton, W. A.; Muñoz, V.; Hagen, S. J.; Jas, G. S.; Lapidus, L. J.; Henry, E. R.; Hofrichter, J. *Annu. Rev. Biophys. Biomol. Struct.* **2000**, *29*, 327–359.
(5) Hagen, S. J.; Hofrichter, J.; Szabo, A.; Eaton, W. A. *Proc. Natl. Acad. Sci. U.S.A.* **1996**, *93*, 11615–11617.
(6) McGimpsey, W. G.; Chen, L.; Carraway, R.; Samaniego, W. N. *J. Phys. Chem. A* **1999**, *103*, 6082–6090.
(7) Möglich, A.; Krieger, F.; Kiefhaber, T. *J. Mol. Biol.* **2005**, *345*, 153–162.
(8) Fierz, B.; Satzger, H.; Root, C.; Gich, P.; Zinth, W.; Kiefhaber, T. *Proc. Natl. Acad. Sci. U.S.A.* **2007**, *104*, 2163–2168.
(9) Möglich, A.; Joder, K.; Kiefhaber, T. *Proc. Natl. Acad. Sci. U.S.A.* **2006**, *103*, 12394–12399.
(10) Hudgins, R. R.; Huang, F.; Gramlich, G.; Nau, W. M. *J. Am. Chem. Soc.* **2002**, *124*, 556–564.
(11) Huang, F.; Hudgins, R. R.; Nau, W. M. *J. Am. Chem. Soc.* **2004**, *126*, 16665–16675.
(12) Roccatano, D.; Sahoo, H.; Zacharias, M.; Nau, W. M. *J. Phys. Chem. B* **2007**, *111*, 2639–2646.
(13) Bieri, O.; Wirz, J.; Hellrung, B.; Schutkowski, M.; Drewello, M.; Kiefhaber, T. *Proc. Natl. Acad. Sci. U.S.A.* **1999**, *96*, 9597–9601.
(14) Krieger, F.; Fierz, B.; Bieri, O.; Drewello, M.; Kiefhaber, T. *J. Mol. Biol.* **2003**, *332*, 265–274.
(15) Lapidus, L. J.; Eaton, W. A.; Hofrichter, J. *Proc. Natl. Acad. Sci. U.S.A.* **2000**, *97*, 7220–7225.
(16) Neuweiler, H.; Löllmann, M.; Doose, S.; Sauer, M. *J. Mol. Biol.* **2007**, *365*, 856–869.
(17) Winnik, M. A. *Acc. Chem. Res.* **1985**, *18*, 73–79.
(18) Svirskaya, P.; Danhelka, J.; Redpath, A. E. C.; Winnik, M. A. *Polymer* **1983**, *24*, 319–322.
(19) Boileau, S.; Méchin, F.; Martinho, J. M. G.; Winnik, M. A. *Macromolecules* **1989**, *22*, 215–220.
(20) Ghiggino, K. P.; Snare, M. J.; Thistlethwaite, P. J. *Eur. Polym. J.* **1985**, *21*, 265–272.
(21) Cheung, S.-T.; Winnik, M. A.; Redpath, A. E. C. *Makromol. Chem.* **1982**, *183*, 1815–1824.
(22) Slomkowski, S.; Winnik, M. A. *Macromolecules* **1986**, *19*, 500–501.
(23) Kim, S. D.; Torkelson, J. M. *Macromolecules* **2002**, *35*, 5943–5952.
(24) Gardinier, W. E.; Bright, F. V. *J. Phys. Chem. B* **2005**, *109*, 14824–14829.
(25) Duhamel, J.; Khayakin, Y.; Hu, Y. Z.; Winnik, M. A.; Boileau, S.; Méchin, F. *Eur. Polym. J.* **1994**, *30*, 129–134.
(26) Lee, S.; Winnik, M. A. *Macromolecules* **1997**, *30*, 2633–2641.
(27) Lee, S.; Duhamel, J. *Macromolecules* **1998**, *31*, 9193–9200.
(28) Farinha, J. P. S.; Piçarra, S.; Miesel, K.; Martinho, J. M. G. *J. Phys. Chem. B* **2001**, *105*, 10536–10545.
(29) Piçarra, S.; Gomes, P. T.; Martinho, J. M. G. *Macromolecules* **2000**, *33*, 3947–3950.
(30) Costa, T.; Seixas de Melo, J.; Burrows, H. D. *J. Phys. Chem. B* **2009**, *113*, 618–626.
(31) Ingratta, M.; Hollinger, J.; Duhamel, J. *J. Am. Chem. Soc.* **2008**, *130*, 9420–9428.
(32) Cuniberti, C.; Perico, A. *Eur. Polym. J.* **1977**, *13*, 369–374.
(33) Cuniberti, C.; Perico, A. *Prog. Polym. Sci.* **1984**, *10*, 271–316.
(34) Winnik, M. A.; Basu, S. N.; Lee, C. K.; Saunders, D. S. *J. Am. Chem. Soc.* **1976**, *98*, 2928–2935.
(35) Horie, K.; Schnabel, W.; Mita, I.; Ushiki, H. *Macromolecules* **1981**, *14*, 1422–1428.
(36) Lee, S.; Winnik, M. A. *Can. J. Chem.* **1993**, *71*, 1216–1224.
(37) Lee, S.; Winnik, M. A. *Can. J. Chem.* **1994**, *72*, 1587–1595.
(38) Birks, J. B. *Photophysics of Aromatic Molecules*; Wiley: New York, 1970; p 301.
(39) Siu, H.; Duhamel, J.; Pincus, J.; Sasaki, D. *Langmuir* **2010**, *26*, 10985–10994.
(40) Mathew, H.; Siu, H.; Duhamel, J. *Macromolecules* **1999**, *32*, 7100–7108.
(41) Duhamel, J. *Acc. Chem. Res.* **2006**, *39*, 953–960.
(42) Press, W. H.; Flannery, B. P.; Teukolsky, S. A.; Vetterling, W. T. *Numerical Recipes. The Art of Scientific Computing (Fortran Version)*; Cambridge University Press: Cambridge, U.K., 1992.
(43) Nakajima, A. *J. Lumin.* **1976**, *11*, 429–432.
(44) Kalyanasundaram, K.; Thomas, J. K. *J. Am. Chem. Soc.* **1977**, *99*, 2039–2044.
(45) Lianos, P.; Georghiou, S. *Photochem. Photobiol.* **1979**, *30*, 355–362.
(46) Dong, D. C.; Winnik, M. A. *Photochem. Photobiol.* **1982**, *35*, 17–21.
(47) Dong, D. C.; Winnik, M. A. *Can. J. Chem.* **1984**, *62*, 2560–2565.

(48) Zachariass, K. A.; Vaz, W. L. C.; Sotomayor, C.; Kühnle, W. *Biochim. Biophys. Acta* **1982**, *688*, 323–332.
(49) Ingratta, M.; Mathew, M.; Duhamel, J. *Can. J. Chem.* **2010**, *88*, 217–227.
(50) Pattanayek, S. K.; Juvekar, V. A. *Macromolecules* **2002**, *35*, 9574–9585.
(51) Bandrup, J.; Immergut, E. H.; Grulke, E. A. *Polymer Handbook*, 4th ed.; John Wiley & Sons: New York, 1999; p VII 675−683.